



ELSEVIER

Available online at [www.sciencedirect.com](http://www.sciencedirect.com)

SCIENCE @ DIRECT®

International Journal of  
**Multiphase  
Flow**

International Journal of Multiphase Flow 30 (2004) 139–157

[www.elsevier.com/locate/ijmulflow](http://www.elsevier.com/locate/ijmulflow)

# Experimental studies on the dual continuous flow pattern in oil–water flows

J. Lovick, P. Angeli \*

*Department of Chemical Engineering, University College London, Torrington Place, London WC1E 7JE, UK*

Received 15 November 2001; received in revised form 24 November 2003

---

## Abstract

The dual continuous flow pattern (both phases retain their continuity at the top and bottom of the pipe while there is interdispersion), which occurs during the pipe flow of two immiscible liquid phases, was studied in detail, and pressure gradient, in situ volume fraction and phase distribution data were obtained. The experimental work was performed in a 38 mm diameter, horizontal, stainless steel test section, using water and oil (6 mPa s viscosity and 828 kg/m<sup>3</sup> density) as test fluids. The identification of the dual continuous flow pattern boundaries was achieved with the use of an impedance and a conductivity probe. Measurements were made for mixture velocities from 0.8 to 3 m/s and input oil volume fractions from 10% to 90%. Dual continuous flow appeared at intermediate mixture velocities between stratified and dispersed flows and resulted in pressure gradients less than those of single phase oil flow; the velocity ratio increased with increasing input oil fraction, and was above 1 at high oil fractions apart from the highest mixture velocities where it was reduced to values below 1. This behaviour was explained by the in situ phase distribution data and the shape of the oil–water interface. The standard two-fluid model was unable to predict the pressure gradient and hold-up during dual continuous flow.

© 2004 Elsevier Ltd. All rights reserved.

*Keywords:* Liquid–liquid flow; Dual continuous; Pressure gradient; Hold-up; Phase distribution

---

## 1. Introduction

Although multiphase flows often involve the presence of two immiscible liquids, the existing literature covers mainly gas–liquid systems with relatively few references to liquid–liquid flows. Even when two liquids are present, usually an organic and an aqueous phase, they are often

---

\* Corresponding author. Tel.: +44-20-7679-3832; fax: +44-20-7383-2348.  
E-mail address: [p.angeli@ucl.ac.uk](mailto:p.angeli@ucl.ac.uk) (P. Angeli).

considered, for design purposes, as one phase with averaged properties (based on the homogeneous model). Flow of two immiscible liquids is common in the petrochemical (during oil production and transportation) and process (some examples include emulsification and extraction) industries either on its own or as part of a more complex multiphase system.

There was an initial interest in oil–water flows relevant to petrochemical industries during the 1950s and 1960s (see for example Russell et al., 1959; Charles et al., 1961), mainly concerned with improving pumping requirements during viscous oil transportation by introducing water in the pipelines. This has only recently been followed by a number of publications, possibly encouraged by the increased production from mature oil fields where more water is present and transported with the oil. Furthermore, the need to improve the predictive models for pressure drop and hold-up in multiphase pipelines requires that details of the flow pattern are resolved and all phases present are accounted for.

During horizontal oil–water flow, the *stratified pattern* (where the less dense phase, usually oil, flows above the more dense phase, usually water, with a defined interface) will appear at low mixture velocities, while the *dispersed pattern* (where one phase is dispersed as droplets into the continuum of the other phase) will appear at high mixture velocities. At intermediate mixture velocities a combination of these two patterns can appear, with both fluids maintaining their continuity but with each phase dispersed, at various degrees, into the continuum of the other (Fig. 1). Investigators have identified different flow patterns depending on the degree of entrainment of one phase into the other, without, however, providing any qualitative criteria on how to differentiate between them. In order to avoid further ambiguity, the patterns where both phases form continuous layers at the top and bottom of the pipe respectively, separated by an interface, but also contain dispersed drops of the opposite phase at various concentrations, are classified in this paper as *dual continuous flow*. Any further subdivisions would depend on detailed knowledge of the degree and height of the dispersion of one phase into the other which is difficult to obtain. Dual continuous flow appears to be very common for a wide range of mixture velocities and input oil volume fractions especially with low viscosity oils.

The well defined interface has allowed experimental and theoretical investigations of stratified flows (Brauner and Moalem Maron, 1989; Kurban, 1997; Ng et al., 2001), while dispersed flow studies (Hinze, 1955; Karabelas, 1978; Angeli and Hewitt, 2000a) have benefited from the extensive work on liquid–liquid dispersions formed in stirred tanks, which offers insight on the mechanism of drop formation and emulsion viscosity. In contrast, little experimental information is available for the dual continuous flow pattern, documenting mainly its boundaries (Table 1). Even more sparse are the modelling attempts, where two approaches have been followed; in the first, the flow is split into three layers, namely clear oil, clear water and dispersed (Guzhov and Medvedev, 1971; Vedapuri et al., 1997), while in the second, the flow is split into two dispersed layers, namely oil continuous and water continuous (Jayawardena et al., 2000; Lovick and Angeli, 2001a).

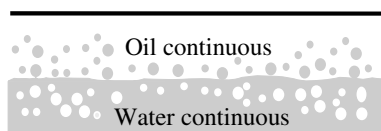


Fig. 1. Schematic diagram of dual continuous flow.

Table 1  
Summary of experimental studies on dual continuous flow

Authors	Pipe ID (mm)	Pipe material	Oil properties			Dual continuous boundaries		Observed dual continuous flow patterns	Flow pattern identification method	Other measured parameters
			$\mu$ (mPa s)	$\rho$ (kg/m <sup>3</sup> )	$\sigma$ (mN/m)	Min mixture velocity oil %	Max mixture velocity oil %			
Guzhov et al. (1973)	39.4	Steel	21.8	896	44.8	0.3 m/s, 30–90%	1.6 m/s, 70–90%	Sep. flow with disp. at int. and water or oil/water bottom layer, emulsion of water/oil and oil/water	Visual observation	$\Delta P$
Malinowsky (1975)	38.4	Steel	4.6	850	22.3	0.6 m/s, 55%	2 m/s, 55%	Do/w and w/o	Visual observation	
Laffin and Oglesby (1976)	38.4	Steel	4.94	828	22.3	0.5 m/s, 43–64%	1.2 m/s, 58%	Segregated, Do/w and w/o	Visual observation	
Oglesby (1979)	41		32	868	30.1		1.4 m/s, 74%	Semi-segregated, Semi-mixed		
Cox (1985), Scott (1985)	50.1	Acrylic	1.38	754		0.7 m/s, 30–76%	1 m/s, 30–76%	Stratified bubble	Visual observation	Hold-up
Trallero (1995)	50.1	Acrylic	29.6	850	36	0.25 m/s, 5–95%	>3 m/s, 50–62%	ST and MI, Do/w and Dw/o	Visual observation	$\Delta P$ , Hold-up
Valle and Kvandal (1995)	37.5	Glass	2.3	794	37.3	0.85–0.9 m/s, 24–68%	1.7 m/s >64% <28%	Stratified wavy-entrain, Stratified wavy with oil and water dispersed zones	Conductivity and sample probes	$\Delta P$  Dispersed layer height

Table 1 (continued)

Authors	Pipe ID (mm)	Pipe material	Oil properties			Dual continuous boundaries		Observed dual continuous flow patterns	Flow pattern identification method	Other measured parameters
			$\mu$ (mPa s)	$\rho$ (kg/m <sup>3</sup> )	$\sigma$ (mN/m)	Min mixture velocity oil %	Max mixture velocity oil %			
Nädler and Mewes (1997)	59	Perspex	22–35	841		0.3 m/s, 20–95%	1.6 m/s, 60%	Stratified with mixing at int., Layers of w/o & w or w/o, o/w & w	Conductivity probe	$\Delta P$
Vedapuri et al. (1997)	101.2	Plexi-glass	2.0			0.4 m/s, 20–80%	1.4 m/s, 20–80%	Semi-segragated, Semi-mixed	Isokinetic probe	Dispersed layer height
Angeli (1996)	24.3	St. Steel	1.6	801	17.0	0.3 m/s, 32–77%	1.3 m/s, 66%	Stratified wavy/drops, Three-layer	Mainly visual observation, Impedance probe	$\Delta P$
Angeli and Hewitt (2000b)	24	Acrylic	1.6	801		0.3 m/s, 33%	1.6 m/s, 50%			Phase distribution
Soleimani (1999)	24.3	St. Steel	1.6	801	17.0	0.5 m/s, 20–85%	1.5 m/s, 62–66%	Stratified wavy/drops, Three-layer	Visual obs., Impedance probe-Gamma densitometer	$\Delta P$ , Hold-up, Phase distribution

The experimental studies on dual continuous flow are summarised in Table 1, which also gives the different names used by the investigators for the patterns that can be classified as dual continuous flow. Guzhov et al. (1973) identified in their study an *emulsion of water/oil and oil/water* (Do/w and Dw/o), a *separate flow with a thick layer of emulsion at the interface with a lower layer of water* and a *separate flow with a thick layer of emulsion at the interface with a lower layer of dilute emulsion o/w*, which are understood to be dual continuous flow. At low mixture velocities and for increasing oil fraction, the pressure drop reached a maximum at about 40% oil during the transition from water continuous dispersed patterns to separate flow with a thick layer of emulsion, while at high mixture velocities this maximum disappeared and a new one was reached at about 70–90% oil, during Do/w and Dw/o; at intermediate mixture velocities both maxima existed.

Cox (1985) and Scott (1985) found that departure from stratified wavy flow and onset of droplet formation at the interface, which signified the start of *stratified bubble* flow (equivalent to dual continuous flow), was marked by a decrease in the interfacial wave amplitude. In all cases of dual continuous flow the velocity ratio (defined as the ratio of the in situ oil to water velocity) was found to be less than one.

Investigations at the University of Tulsa documented a *dispersion of water in oil and oil in water* (Dw/o and Do/w) at higher velocities as well as a *stratified with mixing at the interface* (ST and MI) pattern at lower velocities, both of which can be classified as dual continuous flow (Malinowsky, 1975; Laffin and Oglesby, 1976; Oglesby, 1979; Trallero, 1995). Trallero (1995), from an extensive flow pattern study, reported that, within ST and MI flow, as the mixture velocity increased, the amount of each phase dispersed into the other also increased and became more uniformly distributed into the opposite phase. Visual observations revealed drop sizes between 1 and 12 mm in diameter for ST and MI, decreasing to 2–3 mm for Dw/o and Do/w flow. During ST and MI flow, with the addition of water, the pressure gradient decreased, while during Dw/o and Do/w flow, apart from some initial fluctuations, pressure gradient did not vary significantly. In nearly all cases of dual continuous flows, velocity ratios were less than 1, with the lowest values reached at low input oil fractions.

Valle and Kvandal (1995) studied flow patterns in detail with the use of wall mounted conductivity probes and a sampling tube and observed entrainment of one phase into the other and onset of the *stratified wavy-entrained* pattern at a mixture velocity of about 0.85 m/s. At high and low input oil fractions a *stratified wavy with highly dispersed water zone and moderate dispersed oil zone* pattern and a *stratified wavy with highly dispersed oil zone and moderate dispersed water zone* pattern were observed, respectively. All the above patterns can be considered as dual continuous flow, since both phases retained their continuity. The pressure drop decreased with the addition of water until it reached a minimum at about 60% input water fraction and then increased again.

From the flow patterns observed by Nädler and Mewes (1997) the *layers of water-in-oil dispersion and water* and the *layers of water in oil and oil in water dispersion and water* as well as a *stratified flow with mixing at the interface* at lower mixture velocities, are dual continuous flow. At the boundaries of dual continuous flow with oil- and water-continuous dispersed flows, at low and high water fractions, respectively, peaks in pressure drop were observed.

The patterns identified by Vedapuri et al. (1997) can also be considered as dual continuous flow. The investigators divided them into two categories depending on the height of the dispersed layer between the clear oil and water phases, which they obtained with a sampling probe. As the thickness of the dispersed layer increased, flow changed from *semi-segregated* to *semi-mixed*.

When a high viscosity oil (90 mPa s) was used instead of a low viscosity one (2 mPa s), mixing was less intense.

Angeli and Hewitt (2000b) found that both a *three-layer* (with both phases continuous and entrainment of one phase into the other) and a *stratified wavy with drops* flow patterns appeared in a steel pipe at lower mixture velocities than in an acrylic pipe with the same diameter. In the steel pipe, the two-phase pressure gradient during three-layer flow was higher than that of single phase oil or water, while in the acrylic pipe it was lower than the single phase values (Angeli, 1996). Similar observations were also made by Soleimani (1999) who, in the same experimental set-up, found that the velocity ratio during three-layer flow remained above 1.

It would appear that high-viscosity oils cause the dual continuous pattern to extend to lower mixture velocities. There is no systematic effect of pipe diameter on the boundaries of dual continuous flow; this cannot be conclusive, however, given the small range of diameters used and the simultaneous variation of the other flow parameters. The formation of droplets at the oil–water interface during stratified flow and the onset of dual continuous flow, are probably initiated by the relative movement of the two phases, which creates vortices that penetrate the interfacial boundary (Guzhov et al., 1973). Once a droplet has formed, it is subjected to buoyancy forces, which act to return it to its original phase, and inertial forces which try to disperse it throughout the opposing phase. As the flowrates increase, inertial forces also increase until they are greater than gravitational forces, and the dispersed drops tend to spread more uniformly into the opposing phase.

Given the frequency of dual continuous flows, the objective of the work described in the paper was to investigate this pattern in order to further understand it and to obtain data that can be used for model development. In what follows, Section 2 describes the experimental set-up and instrumentation used, Section 3 summarises the experimental results on dual continuous flow pattern boundaries, pressure gradient and hold-up and compares them with those available in the literature and standard predictive correlations, while Section 4 summarises the conclusions.

## 2. Experimental set-up

The experimental work on dual continuous flow was performed in the liquid–liquid pilot scale flow facility shown in Fig. 2. Oil and water are pumped separately from their storage tanks via two variable-area flow meters and are joined at the beginning of the test section via a modified T-junction which ensures minimum mixing. The test pipe consists of two eight meter sections of 38 mm ID stainless steel tube connected by a U-turn; each section is made up of 1 and 2 m pipes joined with tri-clamp connectors designed to give crevice-free connections. This configuration allows instrumentation to be put in-between the tri-clamp connectors at any location along the test pipe. At the end of the first 8-m section there is a 54 cm transparent acrylic pipe through which the flow can be observed. After the test section, the mixture flows to a separator tank equipped with a coalescer (type DC9201 by KnitMesh Ltd.), which promotes coalescence of dispersed drops and allows fast separation of the two phases. The separated phases are then returned to their respective storage tanks. Water and oil (with properties shown in Table 2) were used as test fluids.

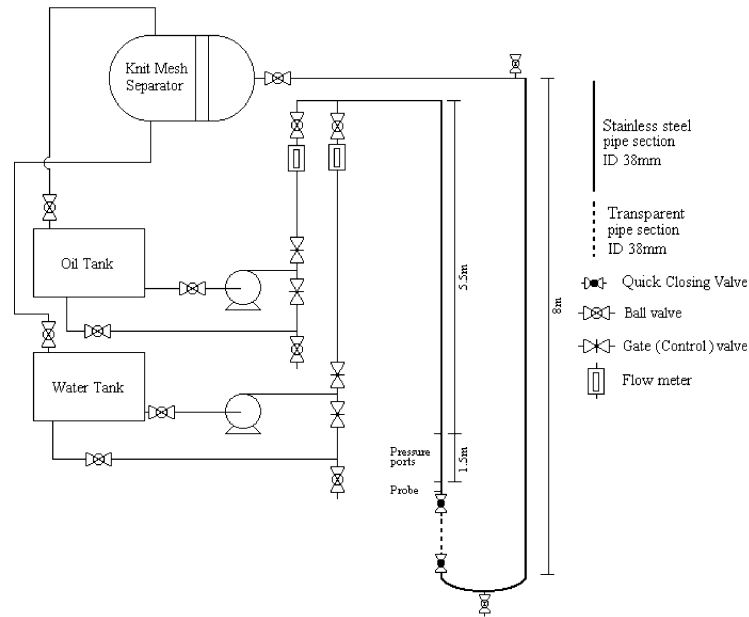


Fig. 2. Diagram of the experimental pilot scale liquid–liquid flow facility.

Table 2  
Oil properties

Product name	EXXSOL D140
Density	828 kg/m <sup>3</sup>
Viscosity	6cP @ 25 °C
Surface tension	27.6 mN/m @ 25 °C
Oil–water interfacial tension	39.6 mN/m @ 25 °C

Flow patterns were identified with a number of techniques. At the lower mixture velocities, the appearance of drops at the oil–water interface and the departure from stratified flow was easily determined by visual observation. At high mixture velocities where visual observation was not sufficient, two probes were used instead; a conductivity probe and a high-frequency impedance probe. The impedance probe gives the distribution of the two phases in a pipe cross section. The conductivity probe provides phase continuity information and shows whether one (dispersed flow) or both (dual continuous flow) phases are continuous.

The impedance probe (for details see Lovick and Angeli, 2001b) consists of a coaxial two-electrode tip, where the inner electrode has a 0.2 mm diameter and the outer one has 0.55 mm ID and 0.175 mm thickness. The two electrodes are separated by an insulator. Due to its small tip size, the probe allows local volume fraction measurements at a point within the test section. Sampling at many points in a pipe cross section gives the phase distribution of oil and water. An alternating current at 7000 Hz frequency was used and a total of 20,000 samples (which corresponds to 2.9 s sampling time) were collected at each sampling point. The probe gives the time (in microseconds) that oil is present at the probe tip for each of the samples, from which the local oil fraction can be

determined. In total, 80 points were sampled at a pipe cross section along four diameters (at 0°, 45°, 90° and 135° from the vertical); samples were taken along a diameter every 2 mm, starting at 0.5 mm from the pipe wall. By integrating the local volume fractions at all points, the average volume fraction of each phase in a pipe cross section can be found. The sampling frequency was found to be sufficient for the experimental conditions used in this work; higher mixture velocities would require higher frequencies (Lovick and Angeli, 2001b). Local volume fractions compared very well with those obtained at longer sampling times of 30 s (equivalent to 210,000 samples) with an average difference less than 1.3% oil volume fraction, indicating that the choice of sampling time was appropriate for the current conditions. The accuracy of the results also depends on the minimum drop size that the probe can detect, which is related to the distance between the two electrodes, equal to 0.175 mm. In dispersed flows it is not possible to calculate the minimum drop size, while investigators have argued that in turbulent systems this should be larger than the Kolmogoroff length scale. In the present work, and for the mixture velocities where the probe was used, this scale was found to be of the order of 100  $\mu\text{m}$ , which indicates that the probe should be able to detect even the small drops present. Moreover, the average oil volume fractions from the impedance probe compared well with the results obtained using quick closing valves (QCVs) with an average difference for all conditions less than 5.8%.

The conductivity probe consists of two 0.5 mm diameter wires, which are placed 10 mm apart in the flow direction, in a vertical position. Each wire is insulated, leaving only a 1 mm long tip exposed to the flow. Both wire tips are located at the same height and can be moved together in the vertical direction from bottom to top of the pipe. By moving the probe vertically, changes in phase continuity can be recorded, which in dual continuous flow will indicate location of the interface. Measurements with both the conductivity and impedance probes were conducted at the same location, 7 m from the beginning of the test section, before the transparent pipe.

The pressure drop was recorded using a differential pressure transducer (Validyne DP103 with an accuracy of 55 Pa) with tapping ports located 1.5 m apart, before the transparent pipe (see Fig. 2). Average in situ phase volume fractions were also measured with QCVs. The valves are placed at each end of the transparent pipe, with a trapped liquid volume of 800 ml (Fig. 2).

Experiments were performed for mixture velocities from 0.8 to 3 m/s and volume fractions from 10% to 90% input oil, the region where initial measurements had shown that dual continuous flow appeared. The full set of experimental data for pressure gradient and average in situ hold up is presented in Table 3. In all experimental runs, the pipe was prewetted with oil before the two-phase mixture was introduced and measurements were taken. Initial experiments showed some differences in the pressure gradient between oil- and water-prewetted pipes, while it has been indicated in the literature that prewetting can affect two-phase flow (Angeli and Hewitt, 1997). It was considered therefore necessary to follow the above procedure for consistency in the results.

### **3. Experimental results**

#### *3.1. Flow pattern map*

The different flow patterns observed at the flow conditions investigated can be seen in Fig. 3 in terms of mixture velocity against input oil volume fraction. Drops of one phase into the other and



Table 3

Panel A: Experimental pressure gradient data (kPa/m); Panel B: experimental in situ oil volume fraction data (%)

% Oil	Mixture velocity (m/s)					
	0.8	1	1.5	2	2.5	3
<i>Panel A</i>						
100	0.220	0.367	0.743	1.328	1.630	2.538
90	0.190	0.292	0.528	1.141	1.584	2.437
86				1.033	1.465	2.038
84				0.779	0.971	2.173
82				0.813	0.901	1.692
80	0.203	0.223	0.448	0.621	0.974	1.670
78				0.679	1.073	1.397
76	0.199	0.230	0.577	0.751	0.980	1.436
74				0.789	1.009	1.251
72	0.177	0.254	0.561	0.850	1.002	1.528
70				0.919	1.261	1.992
68	0.190	0.270	0.597	0.974	1.657	2.011
66				1.029	1.506	1.858
64	0.180	0.292	0.425	0.981	1.439	1.671
62				0.903	1.386	1.911
60	0.180	0.265	0.334	0.929	1.278	1.943
55				0.960	1.475	
50	0.190	0.279	0.392	0.937	1.361	2.064
40	0.183	0.270	0.484	0.936	1.422	2.257
30	0.190	0.286	0.590	1.025	1.605	2.378
20	0.190	0.318	0.629	1.125	1.688	2.403
10	0.196	0.381	0.564	1.205	1.642	2.559
0	0.216	0.301	0.610	1.210	1.600	2.240
<i>Panel B</i>						
90	82.81	83.13	86.56	91.44	92.06	90.63
80	67.19	69.38	75.63	78.75	81.25	81.63
76	64.69	70.00	69.38	73.75	79.88	78.75
72	62.19	63.75	66.25	69.38	75.00	74.75
68	60.63	58.75	61.25	66.05	70.38	70.63
64	56.25	52.50	56.88	62.50	62.50	63.88
60	49.38	51.25	48.75	55.00	59.00	54.38
50	43.44	50.63	43.13	48.13	48.75	50.63
40	33.75	35.00	36.00	39.00	38.75	39.75
30	34.69	20.00	30.63	28.44	28.50	30.00
20	22.19	22.50	30.00	18.13	19.38	19.38
10	13.44	14.38	16.56	9.69	9.69	8.44

the onset of dual continuous flow appeared at 0.8 m/s mixture velocity, with initially only few drops existing at the interface. At lower velocities, *stratified wavy* (SW) flow was observed. The appearance of drops at the oil–water interface coincided with a decrease in the interface wave amplitude of the SW flow. Up to a mixture velocity of 1.5 m/s, dual continuous flow was observed for all input oil fractions used (10–90%). Further increase of the mixture velocity decreased the range of input oil fractions where this pattern appeared, and limited it at the intermediate ones. At

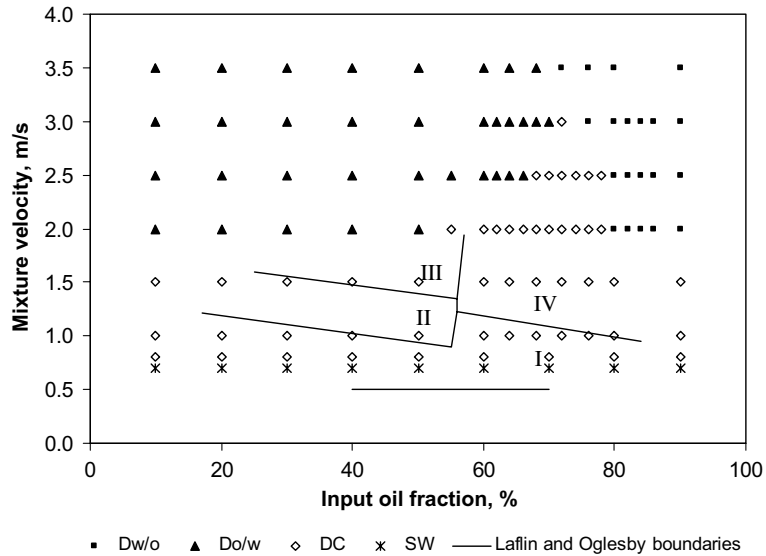


Fig. 3. Comparison of the experimental flow pattern map with the results from Laflin and Oglesby (1976) (solid lines). Regimes defined by Laflin and Oglesby (1976): (I) dual continuous flow; (II) dispersion of oil in water and water; (III) dispersion of oil in water; (IV) dispersion of water in oil.

greater or lesser oil fractions, the flow pattern was *dispersed with oil* (Dw/o) or *water* (Do/w) as the continuous phase, respectively. Above 3 m/s, dual continuous flow did not appear at any oil fraction. At the lower mixture velocities, during the dual continuous regime, the dispersions were mainly concentrated around the interface; as the mixture velocity increased the amount of the dispersed phase within the continuum of the other increased and extended towards the pipe wall.

The dual continuous flow pattern extended to higher mixture velocities than those reported by previous investigators (see Table 1), apart from Trallero (1995), who also identified this pattern at velocities as high as 3 m/s. The reduction in the range of oil fractions at increased mixture velocities, where this pattern appears, has on the other hand been indicated in many previous studies. Only Cox (1985) and Scott (1985) reported that the transition from *stratified bubble* (equivalent to dual continuous) to *massive bubble* (equivalent to dispersed) flow occurred for all oil fractions at the same mixture velocity of 1 m/s, while Vedapuri et al. (1997) also observed dual continuous flow for the whole range of input oil fractions used up to 1.4 m/s.

From the existing flow pattern maps only those by Malinowsky (1975) and Laflin and Oglesby (1976) have been obtained under conditions close to those of the current work (pipe material and diameter and oil density and viscosity). The flow pattern boundaries by Laflin and Oglesby (continuous lines) are plotted together with the current data in Fig. 3. In general, Laflin and Oglesby reported a limited range of conditions where dual continuous flow appeared. It can be seen that the onset of dual continuous flow occurred at lower mixture velocities than in the current study. The onset of dispersed flow also occurred at much lower mixture velocities. Malinowski's data showed that dual continuous flow started at mixture velocities as low as 0.53 m/s. The onset of dispersed patterns at lower velocities than in the current work could be attributed to the lower oil–water interfacial tension (22.3 mN/m in the work by Malinowski and Laflin and Oglesby

compared to 39.6 mN/m in this work). Valle and Kvandal (1995) carried out experiments with similar oil viscosity and pipe diameter, but used a different pipe material (glass) and mixture velocities only up to 1.7 m/s. Dual continuous flow started at approximately 0.8 m/s for high and low input oil fractions, and at approximately 1.2 m/s for the intermediate ones. This suggests that it is probably the increased energy dissipation close to the wall, when the interface is near the bottom or top of the pipe at high and low oil fractions respectively, that increases drop entrainment in stratified flow and causes dual continuous flow to occur at lower mixture velocities at these oil fractions.

### 3.2. Pressure gradient

Pressure gradient data normalised with respect to single phase oil pressure gradient at the same mixture velocity is shown in Fig. 4 for mixture velocities where dual continuous flow appeared. The full set of data is presented in Table 3 (Panel A). The dotted lines indicate dual continuous flow, while the solid lines on the left and right of the dotted lines indicate dispersed water- and oil-continuous flows, respectively.

In general the two-phase pressure gradient was lower than that of single phase oil at the same mixture velocity. At the lowest mixture velocity, where there was only a small amount of dispersion in each continuous phase, there was little variation of the pressure gradient with volume fraction. At the other velocities, the addition of water in single-phase oil resulted initially in a decrease in pressure gradient up to a minimum. With further increase in the water fraction, the pressure gradient increased more sharply at the beginning and then slightly up to the single phase water value. The decrease in pressure gradient from single-phase values could be due to the drag reduction phenomenon that has been observed in dispersed flows. Pal (1993) attributed this phenomenon to the effect that drop breakup and coalescence have on turbulence in unstable

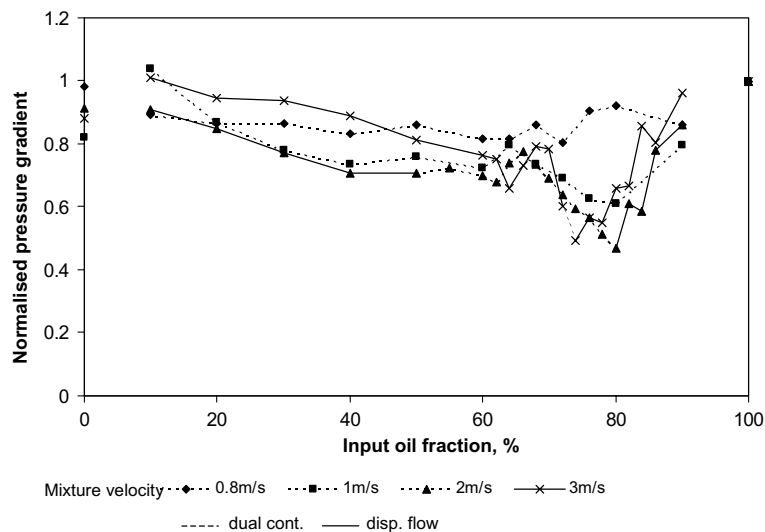


Fig. 4. Experimental normalised pressure gradient against input oil volume fraction at different mixture velocities.

dispersions. It has been observed that the degree of drag reduction increases with dispersed-phase fraction while drag reduction is higher in oil-continuous than in water-continuous flows (Pal, 1993). The minimum in pressure gradient seems to appear at a volume fraction where oil occupies either all (Dw/o at the highest velocities) or a large part (DC at medium velocities) of the pipe and also has a high concentration of dispersed water. At medium velocities, where flow is dual continuous for the whole range of volume fractions, as the water fraction further increases from the minimum point, the water-continuous region grows larger than the oil-continuous region, reducing the overall drag reduction experienced which results in a pressure gradient increase. At the highest velocities, the minimum is associated with the boundary of Dw/o with DC flow and the changes in pressure gradient appear to be more sharp. In these velocities as the water fraction increases beyond the minimum point a separate water continuous layer forms (DC flow) which reduces the amount of dispersion in the oil-continuous phase and also the overall effect of drag reduction.

There are few reported pressure gradient data in the literature for dual continuous flow (see also Table 1). Trallero (1995) for most of the cases studied, Valle and Kvandal (1995) and Nädler and Mewes (1997) also observed a reduction in pressure gradient compared to that of single phase oil during dual continuous flow, similar to the current work. Guzhov et al. (1973), on the other hand, reported that the two-phase mixture pressure gradient, compared to that of single phase oil, increased with the addition of water during ‘water/oil and oil/water emulsion’ flow at high oil fractions, and reached a peak, but decreased during ‘separate flow with emulsion at the interface and a lower layer of emulsion’ flow, at medium oil fractions. Angeli (1996) found that the pressure gradient depended on the pipe material used; in the steel pipe, dual continuous flow resulted in higher pressure gradient, while in the acrylic pipe it resulted in slightly lower pressure gradient than that of single phase oil flow. Changes in the pressure gradient trends during flow pattern transitions have also been reported by other investigators. Nädler and Mewes (1997) observed pressure gradient peaks at the boundaries of dual continuous flow, while Guzhov et al. (1973) also observed a peak at the transition from water continuous dispersed flow to dual continuous flow.

The experimental data was also compared with the two models commonly used to predict pressure gradient in liquid–liquid flows; the two-fluid model (Brauner and Moalem Maron, 1989), suitable for stratified flows, and the homogeneous model, suitable for dispersed flows. In the two-fluid model the momentum balances for each phase are solved to provide pressure gradient and interface height, which gives the average in situ phase volume fraction. Appropriate wall and interfacial shear stresses are needed. In the current work, the wall stress for each continuous phase was set equal to its single-phase flow value, while the interfacial shear stress was taken equal to the wall shear stress of the faster moving phase. In the homogeneous model, the two fluids are assumed to form a mixture that is treated as a single fluid with suitably averaged properties. The mixture density is found from the volume averaged densities of the two phases, while the viscosity is calculated using a viscosity model from the emulsion literature. In the current work, the correlation suggested by Roscoe (1952) and Brinkman (1952), given by Eq. (1), was used. It was chosen against other correlations (e.g. Pal and Rhodes, 1989) which gave similar predictions, as it is easily implemented and also commonly used:

$$\mu_d = \mu_c(1 - \phi)^{-2.5} \quad (1)$$

where  $\mu_d$  is the dispersion viscosity,  $\mu_c$  is the continuous phase viscosity and  $\phi$  is the dispersed phase concentration. In this model, the continuous phase has to be specified for each volume

fraction. The change of phase continuity was assumed to take place at 68% input oil fraction where experiments during dispersed flow at higher mixture velocities and work in stirred vessels indicated that phase inversion appeared.

The comparisons can be seen in Fig. 5 for 1 m/s mixture velocity where the results are normalised with respect to single phase oil. Both models overpredict the experimental pressure gradient data, except at low input oil fractions. For the homogeneous model, the discrepancies could be attributed to the viscosity model used, which does not take into account the observed drag reduction phenomenon. The two-fluid model provides improved predictions, thus confirming the stratified nature of the flow. In this model, however, the interface is assumed flat and no entrainment of one phase into the other is considered. Including these phenomena (i.e. Brauner et al., 1998; Lovick and Angeli, 2001a) could improve the model predictions. The same behaviour was observed at all mixture velocities.

*3.2.1. Velocity ratio and phase distribution*

From the average in situ phase volume fractions (given in Table 3 (Panel B)), obtained from the impedance probe and the QCVs, the ratio *S* of the average in situ oil to water velocity can be found as follows:

$$S = \frac{\text{input oil volume fraction}/\text{input water volume fraction}}{\text{in situ oil volume fraction}/\text{in situ water volume fraction}} \tag{2}$$

Accordingly, *S* is greater than 1 when oil is the faster flowing phase, and conversely *S* is less than 1 when water is the faster flowing phase.

The velocity ratios are plotted against the input oil volume fraction for indicative mixture velocities in Fig. 6. Again, dotted lines indicate dual continuous flow while continuous lines indicate dispersed flows. It can be seen that, in general, as the mixture velocity increases, the

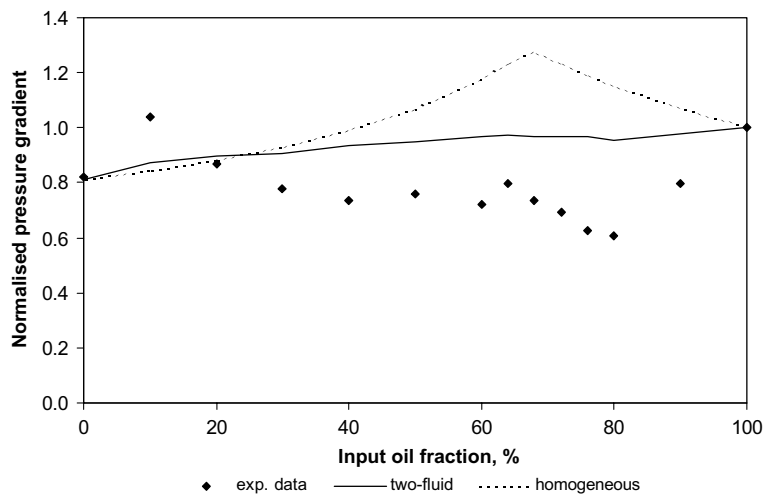


Fig. 5. Comparison of experimental normalised pressure gradient data with the predictions of the two-fluid and the homogeneous models at 1 m/s mixture velocity.

velocity ratio,  $S$ , becomes closer to 1. At mixture velocities greater than 1.5 m/s,  $S$  tends to be greater than 1 at low input oil fractions (where the flow is dispersed with water as the continuous phase), and less than 1 at high input oil fractions (where the flow is dispersed with oil as the continuous phase). This shows that the dispersed phase is flowing faster than the continuous one. However, this trend is reversed at mixture velocities of 1.5 m/s and less, where at low input oil fractions,  $S$  is less than 1, and increases above 1 with increasing oil fractions. At these lower mixture velocities the flow pattern is dual continuous for all input oil fractions, and both oil and water are continuous at the top and bottom of the pipe respectively. As can be seen from the phase volume fraction distribution diagram at 1.5 m/s mixture velocity in Fig. 7(a), at low input oil fractions, the oil forms a thin continuous layer at the top of the pipe with a large wall contact area compared to its volume. The oil therefore experiences large frictional drag, which reduces its velocity compared to that of water and results in  $S$  being less than 1. At high oil fractions (Fig. 7(c)), where the water forms a thin continuous layer at the bottom of the pipe, the opposite is true and the water is now flowing slower, resulting in  $S$  values greater than 1. Although the transition from  $S$  less than 1 to greater than 1 should appear at intermediate oil fractions (as the two-fluid model would also suggest, see Fig. 10), in fact this change appears at oil fractions below 40%. The phase distribution data indicate that at intermediate oil fractions during dual continuous flow, the interface curves upwards and causes the water to have a higher wall contact area than the oil and  $S$  to increase to values above 1 (see Fig. 7(b) for 50% input oil fraction).

During dual continuous flow at high input oil fractions,  $S$  is always greater than 1, apart from the higher two velocities used, namely 2.5 and 3 m/s. In order to explain this change in behaviour, the phase distributions at 68% input oil fraction, for mixture velocities 2 m/s ( $S > 1$ ) and 2.5 m/s ( $S < 1$ ), are shown in Fig. 8(a) and (b), respectively. At 2 m/s, the water is forming a semi-annulus at the lower part of the pipe and has a large contact area with the wall. It is, therefore, experiencing higher frictional drag than the oil, which is able to flow faster ( $S > 1$ ). However, at 2.5 m/s,

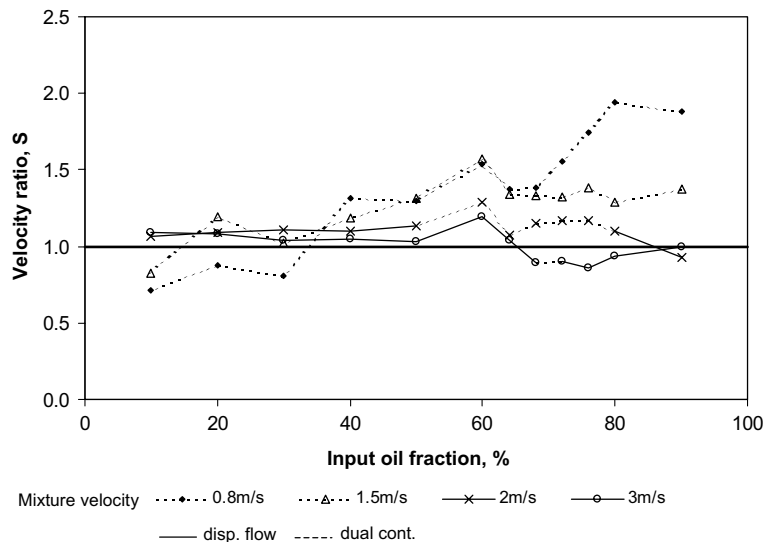


Fig. 6. Experimental velocity ratio data against input oil volume fraction at different mixture velocities.

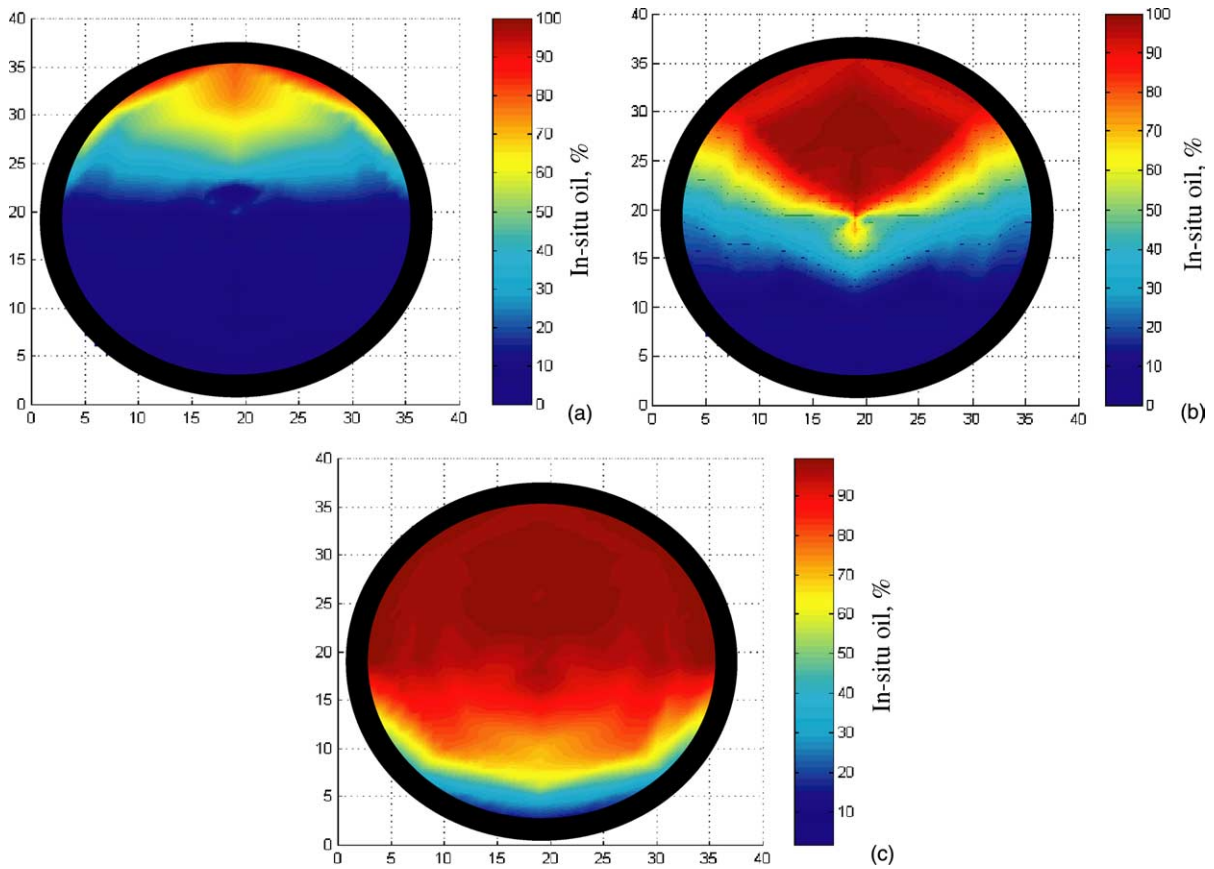


Fig. 7. Oil volume fraction distribution in a pipe cross section at 1.5 m/s mixture velocity: (a) input oil fraction = 20%; (b) input oil fraction = 50%; (c) input oil fraction = 80%.

the water concentration has increased in the faster flowing central region of the pipe, while the oil is now forming a semi-annulus at the top part of the pipe. The oil, therefore, has a large contact area with the wall and experiences high frictional drag, resulting in  $S$  less than 1.

The current results are compared with the available literature data in Fig. 9. Comparisons are made for the same (dual continuous) flow pattern at similar mixture velocities, since in situ hold-up mainly depends on flow pattern. Both Cox (1985)/Scott (1985) (mixture velocities used are 0.88–1.08 m/s) and Trallero (1995) (mixture velocities used are 0.9–1.3 m/s) reported a similar trend to the current work for dual continuous flow, with  $S$  values increasing with increasing input oil fractions. Their  $S$  values, however, did not exceed 1 (apart from few exceptions in the data by Trallero), which could be due to the different pipe material (acrylic) they used compared to the pipe material in the current work (steel). It has been shown (Angeli and Hewitt, 1997) that acrylic is preferentially wetted by oil, which would affect the interface shape and the contact area of the oil with the pipe wall, and could have resulted in higher in situ oil fraction and lower velocity ratio. Of course the different properties of the fluids used in all these investigations could also have affected the distribution of the phases in a pipe cross section and subsequently the velocity ratio.

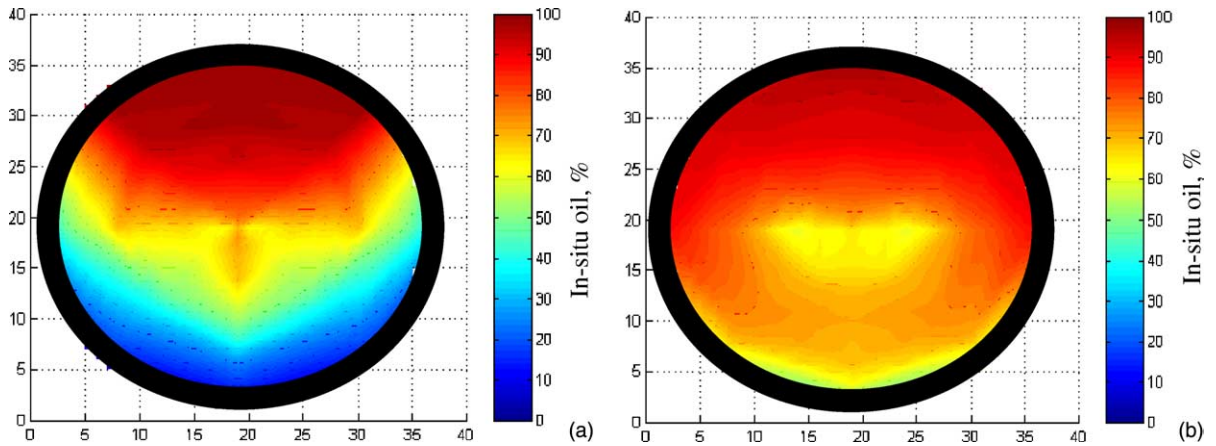


Fig. 8. Oil volume fraction distribution in a pipe cross section for 68% input oil fraction: (a) mixture velocity = 2 m/s; (b) mixture velocity = 2.5 m/s.

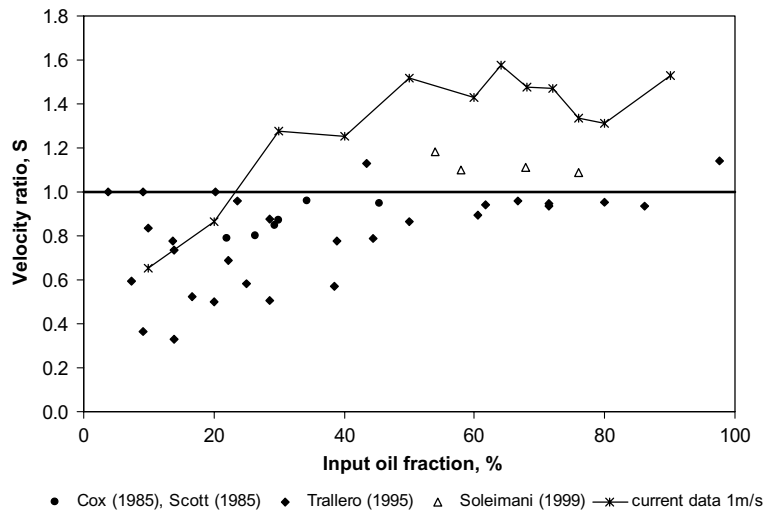


Fig. 9. Comparison of experimental velocity ratios with literature data.

Soleimani (1999) reported hold-up data at a high mixture velocity (1.25 m/s) where dual continuous flow pattern existed at the intermediate input oil fractions (50–74%). For these conditions, his  $S$  values were above 1 during dual continuous flow, in agreement with the current results.

The experimental velocity ratio data is also compared with the two-fluid model predictions in Fig. 10 for 1 m/s mixture velocity. The model is found to underpredict the results, especially at the intermediate oil fractions. This is probably due to the shape of the oil–water interface. The two-fluid model assumes a flat interface, while the phase distribution results from the impedance probe showed a curved interface during dual continuous flow. In particular, at 1 m/s and intermediate



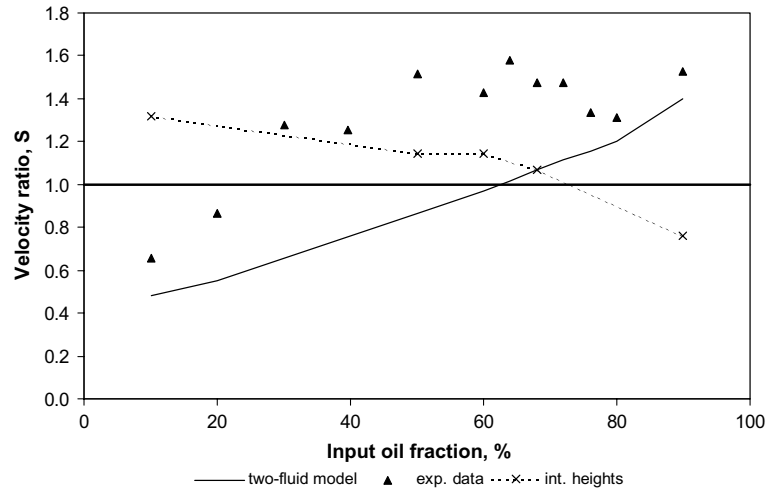


Fig. 10. Comparison of experimental velocity ratio data with those predicted by the two-fluid model and by using the experimentally found interface height at 1 m/s mixture velocity.

oil fractions (where the largest discrepancies between the data and the model occurred), the water forms a semi-annulus surrounding the oil phase (similar to the one at 1.5 m/s in Fig. 7(b)), which then flows faster than the water. Also plotted in Fig. 10 is the velocity ratio calculated using the measured interface height and assuming a flat interface and no entrainment. The discrepancy between the calculated velocity ratios and the experimental data shows that interface height cannot be used for hold-up estimations in dual continuous flows and entrainment has to be taken into account. Comparisons at the other mixture velocities gave similar results.

#### 4. Conclusions

The dual continuous flow pattern during horizontal oil–water flow was studied in detail experimentally, and data on its boundaries, pressure gradient, hold-up and phase distribution were obtained. These revealed the following:

- Dual continuous flow appeared at intermediate mixture velocities for a range of input oil fractions, between the stratified and dispersed patterns.
- In all cases, the addition of water in oil resulted in pressure gradients less than those of single phase oil flow. At the higher mixture velocities, a minimum in the pressure gradient appeared at high oil fractions, perhaps as a combination of the drag reduction phenomenon and the relative fraction of the oil and the water continuous layers in the pipe.
- The velocity ratio increased during dual continuous flow from below 1 to above 1 as the oil input fraction increased. At high input oil fractions, however, the velocity ratio decreased again to values below 1 as the mixture velocity increased. The change of interface shape could explain this behaviour.

- The standard two-fluid model was unable to predict pressure gradient and hold-up during dual continuous flow. Modified versions of the model which take into account the entrainment of one phase into the other and the interface shape need to be developed. The experimental data on phase distribution, obtained in this work, can provide information on entrainment needed by such a model.

## Acknowledgements

J. Lovick would like to thank EPSRC (UK Engineering and Physical Sciences Research Council) for providing financial support for his studentship.

## References

- Angeli, P.A., 1996. Liquid–liquid dispersed flows in horizontal pipes. Ph.D. thesis, Imperial College, University of London.
- Angeli, P.A., Hewitt, G., 1997. Pressure drop measurements in oil and water prewetted pipes. In: Proceedings of the International Symposium on Liquid–Liquid Two-Phase Flow and Transport Phenomena, Antalya Turkey, pp. 75–83.
- Angeli, P., Hewitt, G., 2000a. Drop size distributions in horizontal oil–water dispersed flows. *Chem. Eng. Sci.* 55, 3133–3143.
- Angeli, P., Hewitt, G., 2000b. Flow structure in horizontal oil–water flow. *Int. J. Multiphase Flow* 26, 1117–1140.
- Brauner, N., Moalem Maron, D., 1989. Two phase liquid–liquid stratified flow. *PhysicoChem. Hydrodynam.* 11, 487–506.
- Brauner, N., Moalem Maron, D., Rovinsky, J., 1998. A two-fluid model for stratified flows with curved interfaces. *Int. J. Multiphase Flow* 24, 975–1004.
- Brinkman, H.C., 1952. The viscosity of concentrated solutions and suspensions. *J. Chem. Phys.* 20, 571.
- Charles, M.E., Govier, G.W., Hodgson, G.W., 1961. The horizontal pipeline flow of equal density oil–water mixture. *Can. J. Chem. Eng.* 39, 27–36.
- Cox, A.L., 1985. A study of horizontal and downhill two-phase oil–water flow. M.S. thesis, The University of Texas.
- Guzhov, A.I., Medvedev, O.P., 1971. Pressure losses in flow of two mutually immiscible liquids. *Int. Chem. Eng.* 11, 104–106.
- Guzhov, A.I., Grishan, A.L., Medredev, V.F., Medredeva, O.P., 1973. Emulsion formation during the flow of two immiscible liquids in a pipe. *Neft Khoz.* 8, 58–61 (in Russian).
- Hinze, J.O., 1955. Fundamentals of the hydrodynamic mechanism of splitting in dispersion processes. *AIChE J.* 1, 289–295.
- Jayawardena, S.S., Alkaya, B., Redus, C.L., Brill, J.P., 2000. A new model for dispersed multi-layer oil–water flow. In: Proceedings of the 2000 Multiphase Technology, Banff, Canada, pp. 77–89.
- Karabelas, A.J., 1978. Droplet size spectra generated in turbulent pipe flow of dilute liquid–liquid dispersions. *AIChE J.* 24, 170–180.
- Kurban, A.P.A., 1997. Stratified liquid–liquid flow. Ph.D thesis, Imperial College, University of London.
- Lafin, G.C., Oglesby, K.D., 1976. An experimental study on the effects of flow rate, water fraction and gas–liquid ratio on air–oil–water flow in horizontal pipes. B.S. thesis, The University of Tulsa.
- Lovick, J., Angeli, P., 2001a. Two-phase liquid flows at the partially dispersed flow regime. In: Proceedings of the 4th International Conference on Multiphase Flow, New Orleans, USA.
- Lovick, J., Angeli, P., 2001b. Impedance probe for phase distribution measurements and flow pattern identification in oil–water flows. In: Proceedings of the 5th International Conference on Experimental Heat Transfer, Fluid Mechanics and Thermodynamics, Thessaloniki, Greece.

- Malinowsky, M.S., 1975. An experimental study oil–water and air–oil–water flowing mixtures in horizontal pipes. M.S. thesis, The University of Tulsa.
- Nädler, M., Mewes, D., 1997. Flow induced emulsification in the flow of two immiscible liquids in horizontal pipes. *Int. J. Multiphase Flow* 23, 55–68.
- Ng, T.S., Lawrence, C.J., Hewitt, G.F., 2001. Two-phase stratified flow in an inclined circular pipe. In: *Proceedings of the 4th International Conference on Multiphase Flow*, New Orleans, USA.
- Oglesby, K.D., 1979. An experimental study on the effects of oil viscosity, mixture velocity, and water fraction on horizontal oil–water flow. M.S. thesis, The University of Tulsa.
- Pal, R., Rhodes, E., 1989. Viscosity/concentration relationships for emulsions. *J. Rheol.* 33, 1021–1045.
- Pal, R., 1993. Pipeline flow of unstable and surfactant-stabilised emulsions. *AIChE J.* 39, 1754–1764.
- Roscoe, R., 1952. The viscosity of suspensions of rigid spheres. *Br. J. Appl. Phys.* 3, 267–269.
- Russell, T.W.F., Hodgson, G.W., Govier, G.W., 1959. Horizontal pipeline flow of mixtures of oil and water. *Can. J. Chem. Eng.* 37, 9–17.
- Scott, G.M., 1985. A study of two-phase liquid–liquid flow at variable inclinations. M.S. thesis, The University of Texas.
- Soleimani, A., 1999. Phase distribution and associated phenomena in oil–water flows in horizontal tubes. Ph.D thesis, Imperial College, University of London.
- Trallero, J.L., 1995. Oil water flow patterns in horizontal pipes. Ph.D thesis, The University of Tulsa.
- Valle, A., Kvandal, H., 1995. Pressure drop and dispersions characteristics of separated oil–water flow. In: *International Symposium on Two-Phase Flow Modelling and Experimentation*, Rome, Italy.
- Vedapuri, D., Bessette, D., Jepson, W.P., 1997. A segregated flow model to predict water layer thickness in oil–water flows in horizontal and slightly inclined pipelines. In: *Proceedings of the 8th International Conference on Multiphase Production*, June 18–20, Cannes, France.